Voltage-dependent gating of the Cx32*43E1 hemichannel: Conformational changes at the channel entrances

Taekyung Kwon, Qingxiu Tang, and Thaddeus A. Bargiello

Dominic P. Purpura Department of Neuroscience, Albert Einstein College of Medicine, Bronx, NY 10461

Voltage is an important parameter that regulates the open probability of both intercellular channels (gap junctions) and undocked hemichannels formed by members of the connexin gene family. All connexin channels display two distinct voltage-gating processes, termed loop- or slow-gating and V_j- or fast-gating, which are intrinsic hemichannel properties. Previous studies have established that the loop-gate permeability barrier is formed by a large conformational change that reduces pore diameter in a region of the channel pore located at the border of the first transmembrane domain and first extracellular loop (TM1/E1), the parahelix (residues 42–51). Here, we use cadmium metal bridge formation to measure conformational changes reported by substituted cysteines at loci demarcating the intracellular (E109 and L108) and extracellular (Q56) entrance of hemichannels formed by the Cx32 chimera (Cx32*43E1). The results indicate that the intracellular pore entrance narrows from ∼15 Å to ∼10 Å with loop-gate but not apparently with V_j-gate closure. The extracellular entrance does not appear to undergo large conformational changes with either voltage-gating process. The results presented here combined with previous studies suggest that the loop-gate permeability is essentially focal, in that conformational changes in the parahelix but not the intracellular entrance are sufficient to prevent ion flux.

The Journal of General Physiology

INTRODUCTION

Connexins form both large pore gap junction (intercellular) channels and nonjunctional (undocked) hemichannels that are essential for many physiological and developmental processes and, not surprisingly, the mutational targets of several human diseases (Dobrowolski and Willecke, 2009; Laird, 2010). Voltage is an important regulatory parameter that drives large conformational changes between open and closed states in both intercellular channels and undocked hemichannels. Mutations that alter voltage dependence lead to disease (Oh et al., 1997; Abrams et al., 2000, 2002; Bicego et al., 2006; Lee et al., 2009; Sánchez et al., 2010; Abrams and Scherer, 2012).

Connexin channels display two distinct voltage dependencies, which are termed V_j- or fast-gating and loop- or slow-gating (Trexler et al., 1996; Bukauskas and Verselis, 2004; Bargiello et al., 2012). Both are intrinsic hemichannel processes that appear to have different voltage sensors and gates, and the two processes operate in both intercellular channels (gap junctions) and plasma membrane inserted hemichannels unapposed to another hemichannel (termed undocked or unapposed hemichannels; Trexler et al., 1996; Bargiello and Brink, 2009; Bargiello et al., 2012).

Loop-gating and V_j-gating are defined by the form of gating transitions observed in single channel recordings (Trexler et al., 1996; Bargiello et al., 2012). In brief, V_j-gating corresponds to gating transitions between the fully open and one or more subconductance (residual) states that occur with a time course that cannot be resolved in patch clamp recordings. In macroscopic recordings, hemichannel closure by V_j-gating explains the minimal conductance (G_{min}) observed in conductance-voltage relations of intercellular channels (Bukauskas and Verselis, 2004). Reversal of V_j-gating polarity, by substitution of charged residues or neutralization of existing negative charged residues in the NT of Cx32 and Cx26 (Verselis et al., 1994; Oh et al., 2004), suggests that this domain contains at least a portion of the V_j voltage sensor. The stoichiometry of polarity reversal observed in heteromeric hemichannels containing mixtures of wild-type and polarity-reversing subunits strongly suggests that V_j-gating results from conformational changes in individual subunits rather than by a cooperative (concerted) mechanism involving conformational changes in all six hemichannel subunits (Oh et al., 2000). Conformational changes resulting from closure of V_j-gates are unknown. A V_j-gating model has been proposed in which the Cx26 NT forms a gating particle that occludes the channel pore with no additional conformational changes (Maeda et al., 2009). An alternate

Correspondence to Thaddeus A. Bargiello: ted.bargiello@einstein.yu.edu

Abbreviations used in this paper: AFM, atomic force microscopy; CaCC, calcium-activated chloride channel; CL, cytoplasmic loop; CT, cytoplasmic terminal domain; MTSEA, 2-aminoethyl methanethiosulfonate.

The Rockefeller University Press $30.00
J. Gen. Physiol. Vol. 141 No. 2 243–259
www.jgp.org/cgi/doi/10.1085/jgp.201210839

V_j-gating model has been proposed for Cx43 and Cx32 channels in which the cytoplasmic terminal domain (CT) acts a gating particle to either block the channel pore or to interact with a specific domain in the cytoplasmic loop (CL), which is near the border of the third transmembrane domain, to stabilize the closed channel conformation (Revilla et al., 1999; Moreno et al., 2002; Seki et al., 2004; Shibayama et al., 2006; Bargiello et al., 2012). Deletions of the CT do not remove loop-gating, thus it does not appear that the interaction between the CL and CT plays a role in voltage-dependent loop-gating.

Loop-gating was first described in single channel recordings of undocked Cx46 hemichannels (Trexler et al., 1996). Loop-gate closure is favored at inside negative potentials in all connexin hemichannels examined to date. The closed conformation is stabilized by divalent cations (Verselis and Srinivas, 2008) and is believed to be a mechanism that keeps undocked connexin hemichannels closed to preserve cell integrity before the formation of intercellular channels. A direct voltage-independent action of Ca^{2+} has also been proposed (Unwin and Ennis, 1983, 1984; Bennett et al., 1991; Sosinsky and Nicholson, 2005).

Loop-gating differs from V_j-gating in several ways: (a) The time course of the gating transition from a fully open to a fully closed state is slow, occurring over a time scale of several milliseconds, which is consistent with passage through a series of intermediate, metastable conductance states; (b) loop-gating transitions can result in full channel closure, although partial closures of loop-gates are observed. Qualitatively, residency in intermediate (partially closed) states appears to be voltage-dependent, such that full gating transitions become more frequent with increasing hyperpolarization and the time course of full gating transitions becomes faster (Verselis and Srinivas, 2008); (c) The polarity of loop-gate closure is not reversed by charge substitutions in the NT, which control the polarity of V_j-gate closure; (d) Loop-gate closure is most likely cooperative (concerted), i.e., the six connexin subunits step together through a series of intermediate states to progressively occlude the channel pore (Kwon et al., 2012); (e) Voltage-dependent loop-gating is modulated by extracellular [Ca^{2+}] and [Mg^{2+}], likely by interactions of divalent cations with one or more low-affinity binding sites that stabilize the closed conformation. In most cases, Ca^{2+} has a larger effect on channel gating than does Mg^{2+} (Ebihara et al., 2003; Verselis and Srinivas, 2008). It has been proposed that the site of Ca^{2+} and/or Mg^{2+} binding lies outside the Cx32 (Gómez-Hernández et al., 2003) and Cx46 (Verselis and Srinivas, 2008) hemichannel pore, but based on the Cx26 crystal structure, conserved aspartate (D46) and glutamate (E47) residues that are located within the region of the channel pore that forms at least a portion of the loop-gate permeability barrier (Tang et al., 2009; Verselis et al., 2009) are strong candidates in the formation of a site that coordinates Ca^{2+} and Mg^{2+} with low affinity (see also Zonta et al., 2012).

In addition to modulation of loop-gate voltage dependence (Ebihara et al., 2003; Verselis and Srinivas, 2008), atomic force microscopy (AFM) studies have reported that low extracellular [Ca^{2+}] (0.5 mM) but not Mg^{2+} (2.0 mM) reversibly narrows pore diameter at the extracellular and/or the intracellular entrance of the channel pore of isolated, AFM dissected Cx26 hemichannels in the absence of membrane polarization. Pore diameter was reduced from ∼13–15 to ∼5 Å at a depth of 5 Å from the extracellular channel surface (Müller et al., 2002). This depth corresponds to the pore diameter in the vicinity of the 54th and 55th residue in the Cx26 crystal structure (Maeda et al., 2009) and Cx26 hemichannel equilibrated by all-atom molecular dynamics (Kwon et al., 2011). Extracellular Ca^{2+} was also reported to reduce pore diameter of Cx43 and Cx40 hemichannels reconstituted in DOPC (dioleoyl-phosphatidylcholine) without membrane polarization (Thimm et al., 2005; Allen et al., 2011). Interestingly, extracellular Mg^{2+} concentrations of up to 2 mM had no effect on Cx26 hemichannel pore diameter. This suggests that the closed state induced by the action of Ca^{2+} reported by AFM differs from the voltage-dependent closed state, as the latter is stabilized by millimolar concentrations of both Ca^{2+} and Mg^{2+} (Lopez, W., Y. Liu, A.L. Harris, and J.E. Contreras. 2013. 57th Annual Biophysical Society Meeting. In press.). The relation between the action of Ca^{2+} in loop-gate modulation and its voltage-independent action on isolated or reconstituted connexin hemichannel preparations has not been established.

The central biophysical questions of how voltage couples conformational transitions between open and closed states, as well as the definition of the transition path that connects open and closed states at the atomic level, first and foremost requires knowledge of the atomic structure of open and closed states. The solution of the crystal structure of the Cx26 hemichannel (Maeda et al., 2009), its refinement by all-atom molecular dynamics, and consideration of protein modification by acetylation have provided an atomic model that closely corresponds to the open state (Kwon et al., 2011). Currently, there is no atomic resolution structure of a physiologically relevant connexin channel closed state. A powerful alternative method to define structure is the use of biochemical methods, including chemical cross-linking and disulfide bond and metal bridge formation as molecular rulers to define atomic distance constraints of channel conformations in open and closed states. The distance constraints provide a means to create atomic models that can be validated by comparison of the channel properties derived by application of computational

methods to experimental measurements (Khalili-Araghi et al., 2010, 2012; Vargas et al., 2011).

Our previous studies (Tang et al., 2009), which used state-dependent cadmium-thiolate metal bridge formation and chemical cross-linking of cysteine substitutions of Cx32*43E1 hemichannels, identified a segment (the parahelix, resides 42–51) of the connexin channel pore located at the boundary of the first transmembrane domain and first extracellular loop (TM1/E1) that undergoes a large conformational change with loop-gate closure. The diameter of the channel pore in this region decreased from ∼15–20 Å in the open state to ≤4 Å in the loop-gate closed state, a reduction that would be sufficient to prevent ion flux. Furthermore, this study demonstrated that the structure of the parahelix is reorganized with loop-gate closure and that the TM1/E1 bend angle is likely to straighten. Straightening of the TM1/E1 bend angle is predicted to narrow the cytoplasmic entrance to the channel pore. Overall, similar results were reported for Cx50 undocked hemichannels (Verselis et al., 2009). This study also reported reductions in pore diameter at the 50th residue (51st in Cx50). A central question is whether the loop-gate permeability barrier is focal, i.e., restricted to conformational changes in the parahelix or if conformational changes in other domains also prevent ion flux.

Here, we further define the conformation of the Cx32*43E1 channel pore in the loop-gate closed state by monitoring the state-dependent formation of Cd^{2+}-thiolate metal bridges of cysteine substitutions of residues located at the intracellular and extracellular entrance of this connexin hemichannel. The results show that the intracellular entrance narrows with loop-gate closure. However, the resulting pore diameter (∼10 Å) is unlikely to prevent ionic flux. Furthermore, the extracellular entrance to the channel pore, demarcated by the 56th residue, does not form Cd^{2+}-thiolate bridges and hence does not appear to narrow substantially with voltage-dependent closure by either voltage-dependent process in extracellular solutions containing either 1.8 mM Mg^{2+} or Ca^{2+}.

MATERIALS AND METHODS

Molecular biology

Cx32*43E1 is a chimeric connexin that replaces the first extracellular loop (residues 41–70) of Cx32 with the corresponding Cx43 sequence. Hemichannels formed by the chimera express membrane currents in *Xenopus laevis* oocytes when they are not docked to another hemichannel (Pfahnl et al., 1997; Oh et al., 2000, 2004). Mutations of Cx32*43E1, cloned as an EcoR1 fragment in pGEM7zf (Promega), were produced with QuikChange II Site-Directed Mutagenesis kits (Agilent Technologies) and sequenced in their entirety. DNA clones were linearized with HindIII, and RNA was synthesized from this template with an mESSAGE mACHINE T7 promoter kit (Life Technologies; Ambion) and purified using a Megaclear kit (Life Technologies; Ambion). 50–100 nl of purified RNA (∼1 ng/nl) was injected into *Xenopus* oocytes (Xenopus 1). Oocytes were cultured in media containing (in mM): 88 NaCl, 1 KCl, 1.8 $CaCl_2$, 1 $MgCl_2$, and 10 Hepes, pH 7.6, at 12°C. When necessary, oocytes were preinjected with 30 nl of an antisense phosphorothioate oligonucleotide (0.3 pmol/nl) complimentary to *Xenopus* Cx38 (Barrio et al., 1991; Rubin et al., 1992). This antisense oligonucleotide reduces expression of endogenous Cx38 hemichannel oocyte currents within 24–48 h.

Electrophysiological recording

Methods are described in Tang et al. (2009). Bath solution contained (in mM): 100 cesium methanesulfonate (CsMes), 10 Hepes, pH 7.6, and either 1.8 mM $MgCl_2$ or 1.8 $CaCl_2$, as indicated in the text. Indicated [Cd^{2+}] bath solutions were obtained by adding the appropriate volumes of $CdCl_2$ from a 100 mM aqueous stock solution prepared weekly. Deionized water with a resitivity of 18 MΩ · cm (Milli-Q) was used in solution preparation to minimize the presence of contaminating heavy metals. Recording pipette solutions contained 3 M CsCl and 10 mM Hepes, pH 7.6. Pipette resistances were between 0.1 and 0.25 MΩ. A separate ground chamber containing 3 M KCl was connected to the bath chamber with an agar bridge containing 3 M KCl. Membrane currents were recorded with a CA-1B high-performance oocyte clamp (Dagan Corporation) at room temperature. Currents were digitized at a sampling frequency of 5 kHz and filtered at 200 Hz with a low-pass Bessel filter. Time constants were determined by fitting current traces to exponential functions in Clampfit 9.0 (Molecular Devices). When necessary, current traces were decimated 10-fold in Clampfit 9.0 (Axon) to allow fitting of currents with Clampfit software.

Online supplemental material

Fig. S1 presents current-voltage relations of L108C, N2E L108C, and N2E L109C. Figs. S2 and S3 show the sensitivity of the loop-gate of endogenous Cx38 hemichannels to Mg^{2+} and Cd^{2+}, respectively. Fig. S4 shows the sensitivity of the Cx38 V_j-gate to 20 µM Cd^{2+}. Fig. S5 shows the inactivation of calcium-activated chloride channel (CaCC) currents by a train of voltage steps from −10 to −70 mV in a bath solution containing 1.8 mM Ca^{2+}. Online supplemental material is available at http://www.jgp.org/cgi/content/full/jgp.201210839/DC1.

RESULTS

Topology of connexin channels

The intracellular entrance to the Cx26 channel pore is defined by residues at the border of the second transmembrane domain (TM2) and CL (Maeda et al., 2009; Kwon et al., 2011), whereas the extracellular entrance is defined by the position of the 56th residue in the first extracellular domain (E1). The topology of the channel pore in a homology model of Cx32*43E1N2E hemichannel (constructed with MODELLER; Eswar et al., 2006) after equilibration by all-atom molecular dynamics simulation in an explicit fully hydrated POPC membrane (Fig. 1) is essentially identical to that of Cx26. The principle difference is the diameter of the intracellular pore entrance; ∼30 Å in Cx26 and ∼15 Å in Cx32*43E1 N2E after equilibration.

To examine voltage-dependent conformational changes in these regions of the channel pore, we explored state-dependent formation of Cd^{2+}-thiolate metal bridges by

cysteine substitutions at four loci, L106, R107, L108, and E109, that demarcate the intracellular entrance and two residues, Q56 and T55, that demarcate the extracellular entrance to the channel pore.

Because cysteine substitutions at L106 and R107 cause substantial slowing of the time constants of channel opening and closing, these channels display little or no gating at steady-state when experimental paradigms using trains of voltage pulses alternating between −70 and −10 mV are used. Consequently, we focused our attention on L108 and E109. Of the two loci at the extracellular entrance, only Q56C resulted in expression of membrane current attributable to the connexin hemichannel. T55C did not express hemichannel membrane currents.

Cysteine substitutions at these three loci produce hemichannels on both the Cx32*43E1 and Cx32*43E1 N2E backgrounds that display current relaxations with measurable closing and opening time constants when steady-state conditions are attained using trains of voltage steps from −10 to −70 mV. The N2E substitution reverses the polarity of V_j-gating from closure initiated by membrane hyperpolarization to closure with depolarization, but does not alter the negative polarity of loop-gate closure (Fig. S1). This manipulation of V_j-gating polarity allows determination of Cd^{2+}-thiolate metal bridge formation in the open, loop-gate, and V_j-gate closed states.

Experimental rationale

We use two criteria to assess stabilization ("lock") of a channel in a given conformation by Cd^{2+}: changes in peak current and kinetics. If metal bridges are formed only when the channel resides in a closed state then: (1) conductance will be reduced in test paradigms that favor channel closure and (2) the time constants of channel closure will become faster and the time constants of channel opening will become slower as a consequence of the stabilization of the closed state by Cd^{2+} coordination (see Bargiello et al., 2012) when trains of voltage steps that alternately favor channel opening and closing are used (−10 to −70 mV in this study). That is, in the simplest case, the stabilization of the closed state will slow the rate of channel opening, which will be reflected by a shortening of the time constant of channel closure at −70 mV and lengthening of the time constant of channel opening at −10 mV. If metal bridge formation occurs when the channel resides in the open state, then the time constants of channel closure will become slower and the time constants of channel opening will become faster, and peak conductance will increase as a new steady-state is reached. If metal bridges are formed by interactions with cysteines when the channel resides in a higher free energy transition state, then the rate constants of channel opening and closing will both become slower, and this may be reflected in time constants if one rate constant is changed more than the other. These changes in kinetics may be accompanied by a change in conductance, depending on the relation of pore diameter and/or charges lying within the pore of the transition states relative to the fully open state.

Cadmium is a group IIB transition metal with the electronic configuration [Kr]5s04d10. It is a highly polarizable soft ion that complexes with soft donor atoms (S >> N > O) with a preferred coordination number of four reflecting its electronic configuration. The outer shell of Cd^{2+} can accommodate eight electrons, two from the outer shell of each thiolate group. The molecular geometries and relative affinities of Cd^{2+}-thiolate coordinations are well established. The stabilities of Cd^{2+}–cysteine complexes are highly dependent on the number of thiolate groups participating in metal ion coordination. A tetradentate complex in which a single Cd^{2+} interacts with the thiol groups of four cysteine

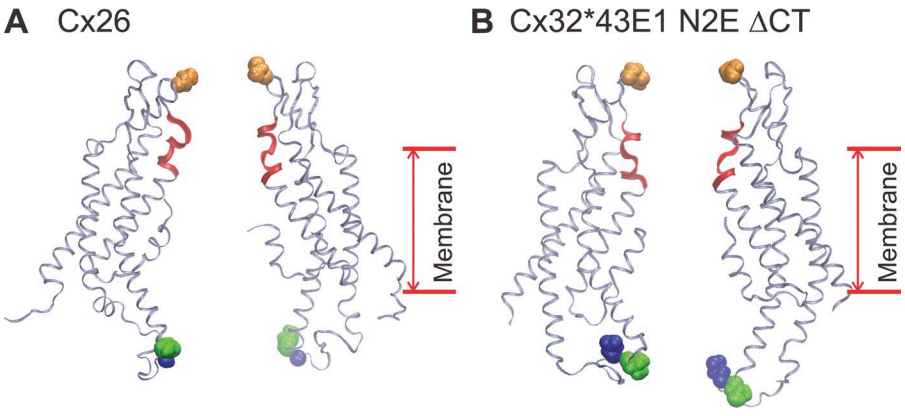

Figure 1. Side view of Cx26 (A) and Cx32*43E1 N2E ΔCT (B) hemichannels after equilibration by all atom molecular dynamics in a fully hydrated POPC membrane. The side chains of residues 108 (green balls), 109 (blue balls), and 56 (orange balls) are shown. The backbone of the parahelix (residues 42–51) is depicted by the red ribbon. The C terminus of Cx32 was not included in the homology model. The Cx32*43E1 N2E hemichannel was incorporated into a fully hydrated POPC membrane as described previously (Kwon et al., 2011). A tetragonal periodic boundary box, 103 × 103 × 109 Å including the protein, lipid membrane, TIP3 waters, and 150 mM KCl, was constructed with a program contained in CHARMM-GUI. All protein atoms in this system used the CHARMM 22 force field with CMAP corrections. The CHARMM 36 force field was used for lipid molecules (Feller and MacKerell, 2000). The system was equilibrated for 1 µs at 310 K using NP_nT dynamics in Desmond using an Anton computer (Shaw et al., 2007). NP_nT is the ensemble name for constant number of particles (N), pressure in normal direction (Pn), and temperature (T).

residues is significantly more stable than a bidentate complex in which a single Cd^{2+} interacts with two cysteine residues (Vilariño et al., 1993; Berthon, 1995). Because the binding energy of cysteines with Cd^{2+} is sensitive to changes in distance, movement of cysteines during gating should introduce a strong energetic bias in favor of residency in a channel state that optimizes the coordination geometry (Holmgren et al., 1998; Yellen, 1998). Formation of either a tetradentate or bidentate coordination site defines the distance separating sulfur and Cα atoms, providing structural constraints to model the closed state: adjacent sulfur atoms are separated by 3.5–4 Å (depending on planar or tetrahedral coordination geometry; see Bargiello et al., 2012) and 5 Å with bidentate coordination; and Cα of coordinating cysteines was separated by 6.5 and 8.2 Å in tetradentate and bidentate coordination, respectively.

Previously, we reported (Tang et al., 2009) that Cd^{2+}-thiolate bridge formation could be reversed by washing with Cd^{2+}-free solutions, or, in one case (A43C), could only be reversed by washing with micromolar concentrations of either DTT or TPEN, both potent Cd^{2+} chelators (Anderegg and Wenk, 1967; Arslan et al., 1985; Krężel et al., 2001). In the case where chelators were required for reversal of Cd^{2+} binding, we demonstrated that a minimum of four cysteine residues was required for high-affinity "irreversible" binding, an observation consistent with tetradentate coordination. We interpreted reversible interactions to reflect the formation of a lower affinity bidentate coordination site by substituted cysteines in neighboring subunits.

Conformational changes at the intracellular entrance reported by E109C

Cd^{2+} stabilizes the loop-gate closed conformation. The effect of a series of Cd^{2+} concentrations (ranging from 10 to 60 µM) on Cx32*43E1 N2E E109C hemichannel loop-gate closure is shown in Fig. 2. Recall that the polarity of V_j-gate closure is reversed by the N2E substitution such that closure of V_j-gates is favored at depolarizing membrane potentials >20 mV (Fig. S1). Current relaxations at hyperpolarizing potentials are a consequence of loop-gating. We have previously reported that Cd^{2+} concentrations ≤100 µM have little effect on voltage-gating of Cx32*43E1 and Cx32*43E1N2E hemichannels (Tang et al., 2009). With the experimental protocol used, alternating steps in membrane potential between −70 and −10 mV, loop-gate closure is strongly favored at −70 mV and opening is favored at −10 mV. The duration of the voltage steps at the two potentials were adjusted to provide stable steady-state currents that were of sufficient magnitude to assess changes in conductance

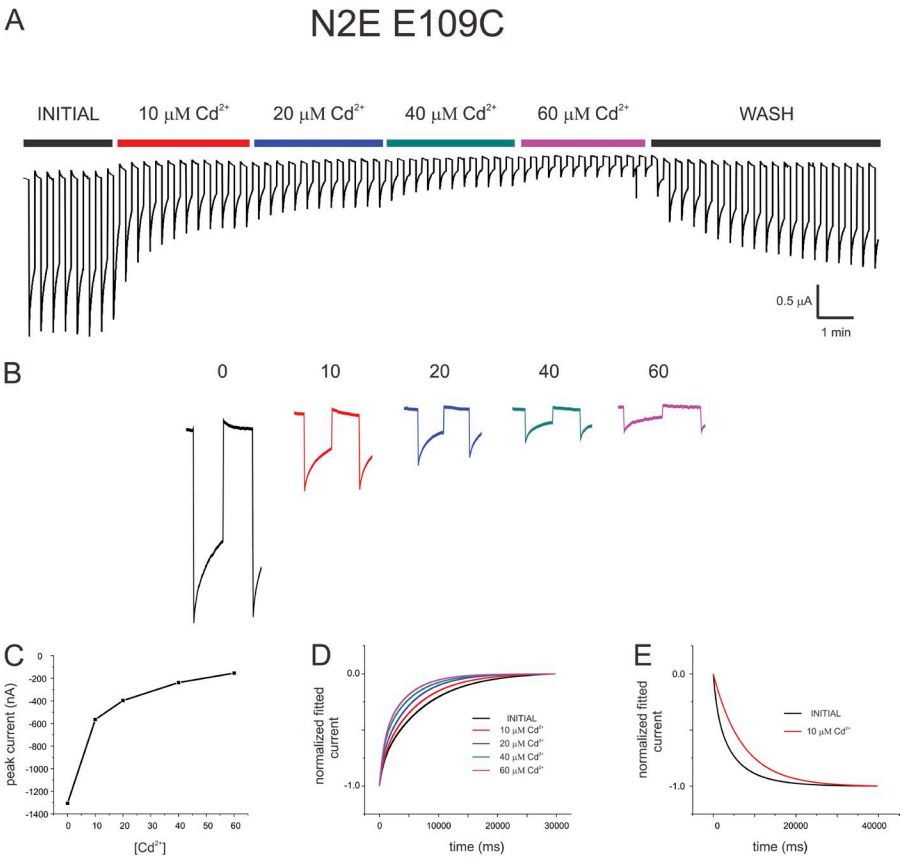

Figure 2. Cadmium stabilizes the loop-gate closed state of Cx32*43E1 N2E E109C hemichannels. (A) A segment of a continuous current trace evoked by a train of alternating voltage polarizations from −10 mV (10 s duration) to −70 mV (10 s duration) with different $[Cd^{2+}]$ indicated by the colored solid bars. (B) Expansion of steady-state current traces shown in A. Current reductions at −70 mV (upward, positive going current relaxations) reflect closure of loop-gates. Increase in currents at −10 mV (downward, negative going current relaxations) reflect opening of loop-gates. (C) Steady-state peak currents measured at −70 mV are plotted against $[Cd^{2+}]$. Half-maximal current reduction is obtained at $[Cd^{2+}]$ ∼10 µM. (D) Plots of normalized fitted currents of steady-state current relaxations at −70 mV. The time constants of current relaxations are shortened as $[Cd^{2+}]$ is increased. Current relaxations were well fitted by standard exponential function with two terms in Clampfit 9.0. (E) Plots of normalized fitted currents of steady-state current relaxations at −10 mV. Current relaxations in 0 and 10 µM Cd^{2+} were well fitted by single exponential functions. Current relaxations obtained with 10-s voltage applications became linear in higher $[Cd^{2+}]$ and could not be fitted to an exponential function.

and to determine time constants of closing and opening in the presence and absence of Cd^{2+}. In the case shown, voltage steps were 10 s at −70 mV and 10 s at −10 mV. Furthermore, records were obtained in Mg^{2+}- rather than Ca^{2+}-containing bath solutions to prevent currents produced by activation of CaCCs that result from influx of extracellular Ca^{2+} through open connexin hemichannels. CaCC currents are activated with depolarization to positive membrane potentials but inactivate rapidly with repeated pulses to negative potentials (Eggermont, 2004; Hartzell et al., 2005; see Fig. S5).

As shown in Fig. 2 A, increasing [Cd^{2+}] progressively decreases connexin current. The time course of this reduction to new steady-state levels reflects the rate of solution exchange with the gravity perfusion system we used and the volume of the bath chamber (∼2 ml). Notably, the effects of Cd^{2+} on connexin currents are immediate. Current traces corresponding to steady-state are shown in Fig. 2 B. Peak currents for this oocyte measured at −70 mV are plotted as a function of [Cd^{2+}] in Fig. 2 C and suggest that the affinity of Cd^{2+} coordination to thiol groups of E109C residues is in the range of 10 µM (the concentration of Cd^{2+} at which currents are reduced by ∼50%). We did not attempt to further quantify K_d because there is a large variation in the amount of current reduction caused by Cd^{2+} among independent experiments performed in different batches of oocytes. For example, the decrease in peak current observed in 10 µM Cd^{2+} varied from ∼60% shown in Fig. 2 to ∼25% in other experiments using different batches of oocytes (not depicted). In 10 µM Cd^{2+}, the mean current reduction was 44 ± 14% (n = 15), 57% ± 20 (n = 6) in 20 µM Cd^{2+}, 73% ± 12 (n = 3) in 40 µM Cd^{2+}, and 74% ± 11 (n = 6) in 60 µM Cd^{2+}. In all cases, we observed a decrease in peak connexin current when Cd^{2+} was applied to Cx32*43E1 N2E E109C channels.

There are several experimental factors that may contribute to the variable effect of Cd^{2+} on peak current. High expression of exogenous Cx32*43E1 hemichannels may reduce the magnitude of applied membrane potentials because of series resistance, thereby altering the proportion of channels residing in open and closed conformations at steady-state. For example, in an oocyte expressing ∼20 µA 109C current at −70 mV, peak current reduction was only 14% in 10 µM Cd^{2+}. Expression of leak and/or nonconnexin currents insensitive to Cd^{2+} would decrease the measured effect of Cd^{2+} on peak connexin current. Trace amounts of heavy metals such as Zn^{2+} in water and salts would also lead to underestimation of current reduction attributed to Cd^{2+} addition. Cx38 is known to contribute to endogenous currents observed in oocytes. These endogenous hemichannel currents are markedly reduced after application of micromolar concentrations of Cd^{2+} and 1.8 mM extracellular Mg^{2+} (Figs. S2–S4). Although, levels of endogenous currents attributable to Cx38 expression are low in most batches of oocytes, and when necessary were further reduced by preinjection of antisense oligonucleotides, expression of low levels of Cx38 would result in overestimation of reductions in peak current contributed by 43E1 hemichannels. We did not perform metal-bridge formation experiments when Cx38 and/or other endogenous oocyte currents exceed 200 nA in uninjected oocytes in recordings obtained in 1.8 mM $MgCl_2$. Peak 43E1 hemichannel currents were typically >5 µA in cadmium-free solutions at −70 mV.

The current relaxations corresponding to channel closure at −70 mV are well fitted by two exponential functions. A progressive shortening of time constants (evident in changes in the time required for fitted normalized current traces to reach steady-state) is observed as [Cd^{2+}] is increased (Fig. 2 D). Changes in time constants of channel closure at −70 mV in solutions containing 10, 20, 40, and 60 µM Cd^{2+} are summarized in Table 1. The slower time constant, tau1 (τ_1), is shortened markedly in Cd^{2+}-containing solutions, from 9.1 ± 1.3 s to 6.5 ± 1.3 s (n = 12) and from 9.0 ± 1.6 s to 4.4 ± 0.6 s in 10 and 60 µM Cd^{2+}, respectively. The differences in time constants, τ_1, are statistically significant in all [Cd^{2+}] ($P > 0.05$, paired sample t test; Origin Pro8; Microcal). Although, the faster time constant, τ_2, is shortened in all paired comparisons, the differences are not statistically

TABLE 1

*Summary of time constants of loop-gate closure at − 70 mV for Cx32*N2E E109C hemichannels*

Amount of Cd^{2+}	Initial		In Cd^{2+}	
	τ_1 (s)	τ_2 (s)	τ_1 (s)	τ_2 (s)
10 µM Cd^{2+} (n = 12)	9.1 ± 1.3	0.68 ± 0.08	6.5 ± 1.3	0.60 ± 0.1
20 µM Cd^{2+} (n = 6)	7.9 ± 1.6	0.70 ± 0.05	5.4 ± 1.3	0.65 ± 0.1
40 µM Cd^{2+} (n = 2)	9.0 ± 2.3	0.7 ± 0.1	5.1 ± 0.4	0.7 ± 0.04
60 µM Cd^{2+} (n = 6)	9.0 ± 1.6	0.7 ± 0.4	4.4 ± 0.8	0.6 ± 0.14

TABLE 2

*Summary of time constants of loop-gate closure at − 70 mV for Cx32*N2E L108C hemichannels*

Amount of Cd^{2+}	Initial		In Cd^{2+}	
	τ_1 (s)	τ_2 (s)	τ_1 (s)	τ_2 (s)
10 µM Cd^{2+} (n = 16)	3.1 ± 0.8	0.45 ± 0.09	1.8 ± 0.3	0.34 ± 0.08
20 µM Cd^{2+} (n = 5)	5.2 ± 2.4	0.50 ± 0.1	2.9 ± 2.0	0.42 ± 0.14
40 µM Cd^{2+} (n = 2)	2.9 ± 0.6	0.5 ± 0.1	1.7 ± 0.3	0.3 ± 0.02

significant for 20, 40, and 60 μM Cd^{2+} with the available sample size, but differ significantly for 10 μM Cd^{2+}.

The lengthening of the time constant of channel opening at −10 mV is shown in Fig. 2 E for 10 μM Cd^{2+}. Current traces corresponding to channel opening at −10 mV are well fitted by a single exponential function. On average, the time constant of channel opening is lengthened from 3.84 ± 0.78 s to 5.49 ± 1.5 s (n = 14) in 10 μM Cd^{2+}. In 20 and 60 μM Cd^{2+}, time constants lengthen from 3.8 ± 0.57 s to 7.1 ± 1.4 s (n = 6) and from 3.1 ± 0.55 s to 6.2 ± 1.3 s, respectively. We could not obtain reliable determinations of time constants in 40 μM Cd^{2+} because of oscillations in the low current levels in these oocytes. The differences in 10, 20, and 60 μM are statistically significant ($P > 0.05$, paired samples t test). In all cases, the time constant of channel opening lengthened for each paired sample in the presence of the given [Cd^{2+}]. Collectively, the shortening of time constants of channel closure at −70 mV, the lengthening of time constants of channel opening at −10 mV, and the marked decrease in peak current is consistent with the Cd^{2+} stabilization of the loop-gate closed state; i.e., Cd^{2+} "locks" the channel in a loop-gate closed conformation.

In the case shown, currents did not fully recover to initial values before the experiment was terminated. However, in experiments of shorter duration, currents and time constants recover fully to their initial values (not depicted). The reversibility of Cd^{2+} treatment is consistent with lower affinity bidentate coordination, most likely involving Cd^{2+} interactions of cysteine residues in adjacent connexin subunits. This constrains the position of adjacent Cα's to 8.2 Å. The distance separating adjacent thiol groups will be ∼5 Å, which sets the minimum pore diameter at ∼10 Å in the loop-gate closed conformation of E109C hemichannels with the assumption of sixfold channel symmetry.

2-aminoethyl methanethiosulfonate (MTSEA) modification of E109C attenuates Cd^{2+} stabilization of the loop-gate closed state. To determine whether the effects of Cd^{2+} on loop-gating were specific to Cd^{2+} interactions with the thiol group of the substituted cysteine, we examined the effect of Cd^{2+} on loop-gating after modification of E109C by MTSEA (Akabas et al., 1992; Karlin and Akabas, 1998). We reasoned that if E109C residues are accessible to MTSEA modification, as indicated by a change in conductance and/or voltage sensitivity, the ability of Cd^{2+} to stabilize the loop-gate closed conformation would be significantly attenuated after the thiol group was modified if backbone N and O atoms did not participate in Cd^{2+} coordination. This is what we observed (Fig. 3). Before MTSEA treatment, 10 μM Cd^{2+} resulted in an ∼30% decrease in peak current relative to the magnitude of currents after washing with Cd^{2+}-free solutions (Fig. 3 A). Application of ∼2 mM MTSEA increased peak currents measured at −70 mV and markedly shortened the time constant of loop-gate closure (Fig. 3 B). The effects of MTSEA application on channel properties did not reverse after its removal by washing,

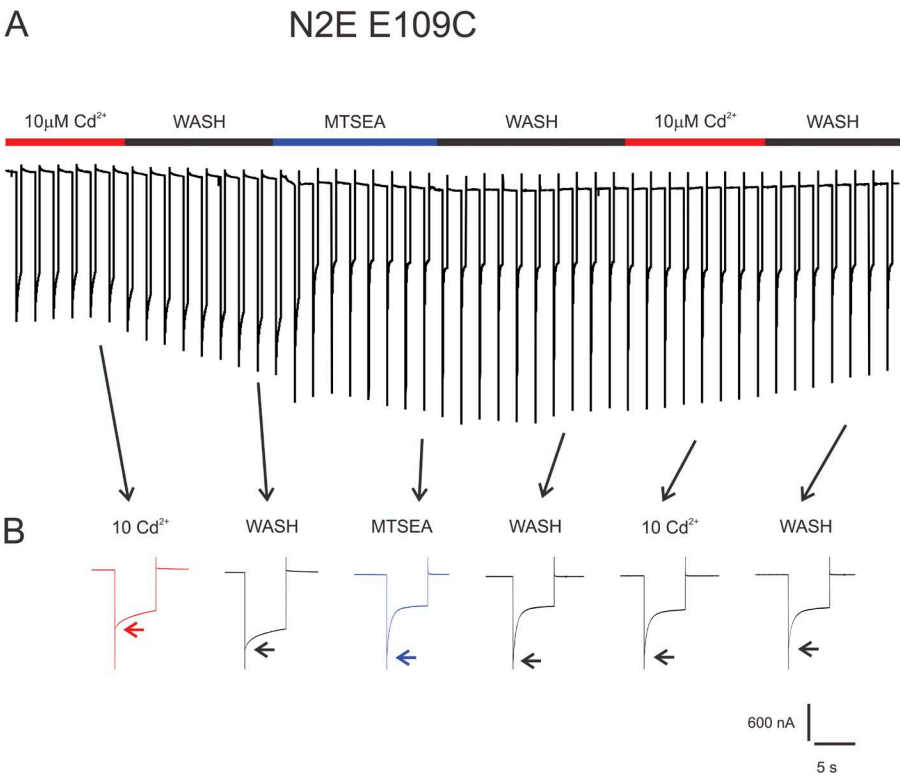

Figure 3. MTSEA modification of E109C attenuates Cd^{2+} stabilization of the loop-gate closed state. (A) A segment of a continuous current trace evoked by a train of alternating voltage polarizations between −10 mV (15 s duration) and −70 mV (5 s duration). The colored solid bars indicate the onset and duration of specified treatments. Capacitive transients were reduced but not fully eliminated by 100× data reduction in Clampfit. (B) Expansion of steady-state current traces shown in A as indicated by arrows. Peak currents obtained at steady-state at −70 mV are marked by arrows.

which is consistent with covalent modification of the thiol group. Subsequent application of 10 μM Cd^{2+} had no or little effect on peak current or on the time constant of loop-gate closure at −70 mV. Notably, peak current continued to decrease slightly after washing with Cd^{2+}-free solutions, which suggests a small rundown of connexin current in this long recording (>20 min). The current trace shown is representative of four experiments. The results strongly suggest that Cd^{2+} stabilizes the loop-gate closed state primarily by coordination with the thiol moiety of E109C residues, and that Cd^{2+} interactions with backbone N and O atoms of E109C have little if any role in coordination.

Endogenous cysteines in the C terminus are not required for Cd^{2+} coordination by 109C. Although there is evidence indicating that the CT–CL interaction, which is required for pH and V_j-gating, is not required for voltage-dependent loop-gating of Cx43 hemichannels (Moreno et al., 2002), we determined whether endogenous cysteines in the CT of Cx32*43E1 participate in the coordination of Cd^{2+} by E109C to stabilize the loop-gate closed state. Cx32*43E1 contains four intracellular cysteine residues: C201 in TM4 and three, C217, C280, and C283, in the CT. C217 is located near the TM4 and CT border ∼50 Å from the pore entrance, and consequently neither it nor C201 could interact with a substituted cysteine at E109 (Fig. 1). It is possible that C280 and C283, which are located at the end of the CT, could interact with substituted cysteines near the cytoplasmic entrance. We explored this possibility by examining Cd^{2+} coordination by N2E E109C hemichannels in which the C terminus was truncated at residue 247 (N2E E109C 247stop). The record shown in Fig. 4 demonstrates that N2E E109C 247stop hemichannels coordinate Cd^{2+} with loop-gate closure in a fashion comparable to that observed for N2E 109C; peak current is reduced by 50% and the time constants of channel closure at −70 mV are shortened in 20 μM Cd^{2+} (initial – τ_1 = 3.93 s, τ_2 = 0.36 s; 20 μM Cd^{2+} – τ_1 = 2.37 s, τ_2 = 0.37 s; wash – τ_1 = 3.47 s, τ_2 = 0.33 s). The time constants of channel opening at −10 mV were well fitted by a single exponential function and indicate lengthening of the time constant of channel opening in the presence of Cd^{2+} (initial – τ = 1.53 s; 20 μM Cd^{2+} – τ = 2.42 s; wash – τ = 1.55 s). We obtained qualitatively similar results in four other oocytes. Thus, substituted cysteines at E109 are sufficient to account for the observed Cd^{2+} stabilization of the loop-gate closed state. There is no evidence that C280 and C283 are involved in metal bridge formation. The results support the view that a CT–CL interaction is not required for loop-gating.

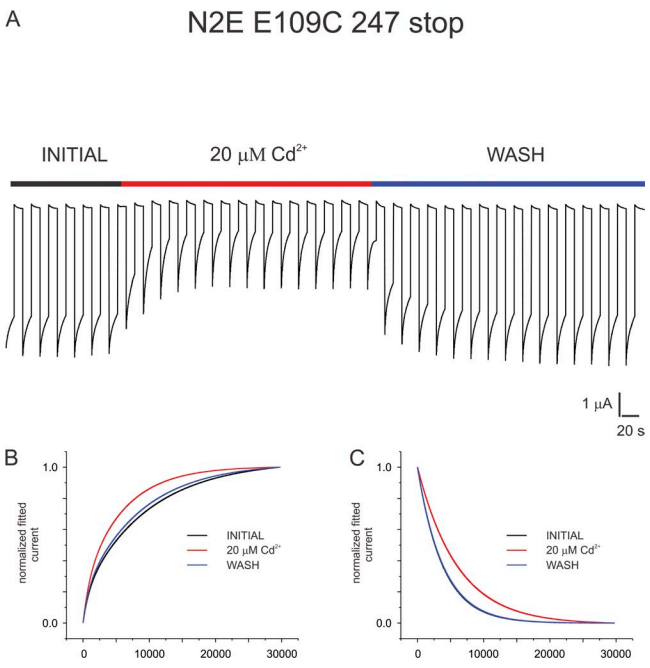

Figure 4. Endogenous cysteines in the CT are not required for Cd^{2+} coordination by E109C. (A) A segment of a continuous current trace evoked by a train of alternating voltage polarizations from −10 mV (10 s duration) to −70 mV (10 s duration). 20 μM Cd^{2+} was applied for the time indicated by the red bar. (B) Plots of normalized fitted currents of steady-state current relaxations at −70 mV corresponding to loop-gate closure. (C) Plots of normalized fitted currents of steady-state current relaxations at −10 mV corresponding to loop-gate opening.

Cd^{2+} does not bridge substituted cysteines with V_j-gate closure. In contrast to loop-gating, V_j-gating of N2E109C is not substantially changed by Cd^{2+}. This is illustrated in Fig. 5, where segments of current traces obtained in a long recording, in which membrane potential was stepped repeatedly between 10 and 50 mV. The current relaxations observed at 50 mV represent closure of V_j-gates, as in this paradigm, loop-gates reside primarily in the fully open state at 10 mV. Notably, there is no marked relaxation of currents at 10 mV after steps to 50 mV, which suggests that opening of V_j-gates at 10 mV is fast.

Perfusion with 20 μM Cd^{2+} does not substantially change peak conductance. The rate of current relaxations with V_j closure become slightly slower, but this time-dependent slowing of V_j closure is often observed even in the absence of Cd^{2+} application (unpublished data). The basis for this phenomenon is unknown but may reflect the activation of low levels of an endogenous current when long trains of voltage polarizations are applied to oocytes. Significantly, the rate of current relaxations caused by V_j closure at 50 mV does not change after Cd^{2+} removal by washing (Fig. 5 A), although peak current increases slightly (Fig. 5, A and B). The slower time constant of channel closure observed in Cd^{2+} (i.e., increase in the time to reach steady-state current) is in any case inconsistent with an action of Cd^{2+} that would stabilize the V_j closed state. The results are representative of experiments performed in six oocytes. A very

small effect of Cd^{2+} is evident in the current trace shown in Fig. 5 D. There, V_j-gate closure was evoked with a membrane depolarization of 40 mV from a holding potential of 10 mV, and 10 µM Cd^{2+} was applied before the current relaxed to steady-state. The small change in the time course of the current relaxation evident after application of Cd^{2+} indicates a small decrease in conductance, but because one cannot ascertain the state-dependence of the effect with this experimental paradigm, stabilization of the loop-gate closed state cannot be distinguished from a slight, slow developing block of the open state by Cd^{2+} or stabilization of an intermediate or "transition" state that connects the open and V_j-closed states. It should also be noted that because closure of the V_j-gate can be accomplished by the movement of a single subunit (Oh et al., 2000), adoption of the V_j-closed conformation may not substantially reduce the distance between adjacent substituted cysteines. Thus, the stabilization of a V_j-closed state by Cd^{2+} may require application of larger voltages that are expected to favor conformational changes in more than a single subunit. In spite of this potential complication, the failure to observe any effect of Cd^{2+} on V_j-gating suggests that the extracellular entrance does not narrow to within 10 Å in the V_j-closed conformation.

However, it should be noted that inside positive potentials would tend to reduce the concentration of Cd^{2+} at the intracellular entrance to the channel pore. Thus, the inference that pore diameter at the extracellular entrance does not change markedly with V_j-gating should be interpreted with caution. However, the presence of appreciable fixed negative charge in the cytoplasmic half of the connexin channel pore and near the intracellular channel entrance predicted by structural models of Cx26 (Maeda et al., 2009; Kwon et al., 2011) and Cx32*43E1 N2E (Fig. 1) may allow Cd^{2+} occupancy at these positions in the channel pore even at positive potentials given a small but near infinite Cd^{2+} gradient.

Cd^{2+} does not appear to coordinate with E109C in the open state. Fig. 6 illustrates the effects of Cd^{2+} on E109C hemichannels. In this mutation, both loop and V_j-gate closures are favored with membrane hyperpolarization,

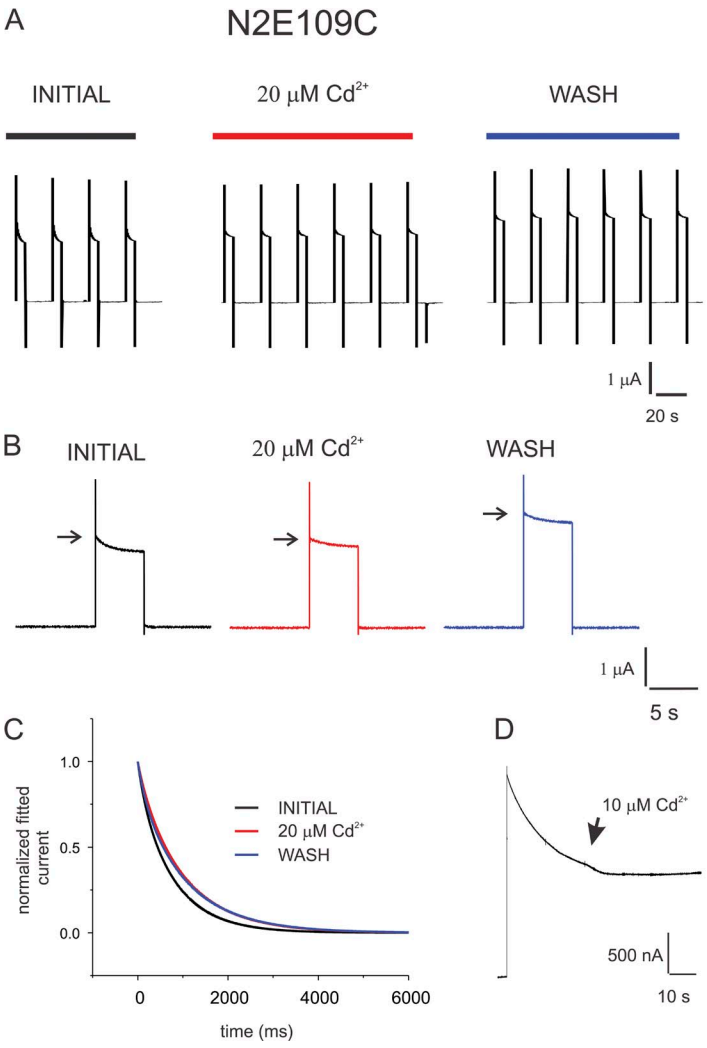

Figure 5. Cd^{2+} does not substantially alter V_j-gating of Cx32*43E1 N2E 109C hemichannels. (A) Segments of a continuous current trace evoked by a train of alternating voltage polarizations from 10 mV (15 s duration) to 50 mV (5 s duration). The current relaxations elicited at 50 mV correspond to the closure of V-gates. The time course of currents elicited at 10 mV is nearly linear and suggests that the time course of V_j-gate opening is fast at this potential. The colored solid bars indicate the onset and duration of the specified treatments. (B) Expansion of steady-state current traces shown in A. Peak currents at 50 mV are marked by arrows. (C) Plots of normalized fitted currents of steady-state current relaxations at 50 mV. Current elicited by a 40-mV polarization. The oocyte was perfused with bath solution containing 10 µM $CdCl_2$ at the time indicated by the arrow. (D) A continuous trace of Cx32*43E1 E109C hemichannel evoked by a 40-mV polarization from a holding potential of 10 mV. The observed current relaxation reflects closure of V_j-gates. 10 µM Cd^{2+} was perfused at the time indicated by the arrow.

and the open state is strongly favored at depolarizing potentials, more positive than −20 mV (unpublished data).

Fig. 6 A shows the effect of 60 µM Cd^{2+} when voltage was stepped from −70 to 10 mV; Fig. 6 B differs only in that voltage in the same oocyte was stepped from −70 to −10 mV. The reduction in peak current measured at−70 mV was much larger when voltage was stepped to −10 mV (a 65% decrease) than when stepped to 10 mV (a 43% decrease). The difference may reflect a voltage dependence of the off rate of Cd^{2+} binding; i.e., greater depolarization increases the rate at which Cd^{2+} dissociates from coordinating thiol groups. Fig. 6 (C and D) shows plots of fitted normalized current relaxations of channel closure at −70 mV for the record shown in Fig. 6 B (−70 to −10 mV polarizations) and of channel opening at −10 mV. The plots, which reflect shortening of the time constant of channel closure and lengthening of the time constant of channel opening, are expected if Cd^{2+} stabilizes the closed state and are consistent with the results obtained for N2E E109C hemichannels showing that Cd^{2+} stabilizes the loop-gate closed state. Similar results were obtained in two additional experiments.

Fig. 6 E demonstrates that 60 µM Cd^{2+} does not reduce conductance when voltage steps between 10 and 50 mV are applied repeatedly. This voltage paradigm is expected to drive all channels into the open state. The slow progressive increase in channel conductance may reflect the development of a small leak current or the incorporation of additional connexin channels into the oocyte membrane at positive potentials during the recording. In other recordings, no change or a small decrease (<10%) in conductance were observed (n = 3 oocytes). We conclude that Cd^{2+} does not interact with E109C when the channel resides in the open state, although as discussed above, the negative result

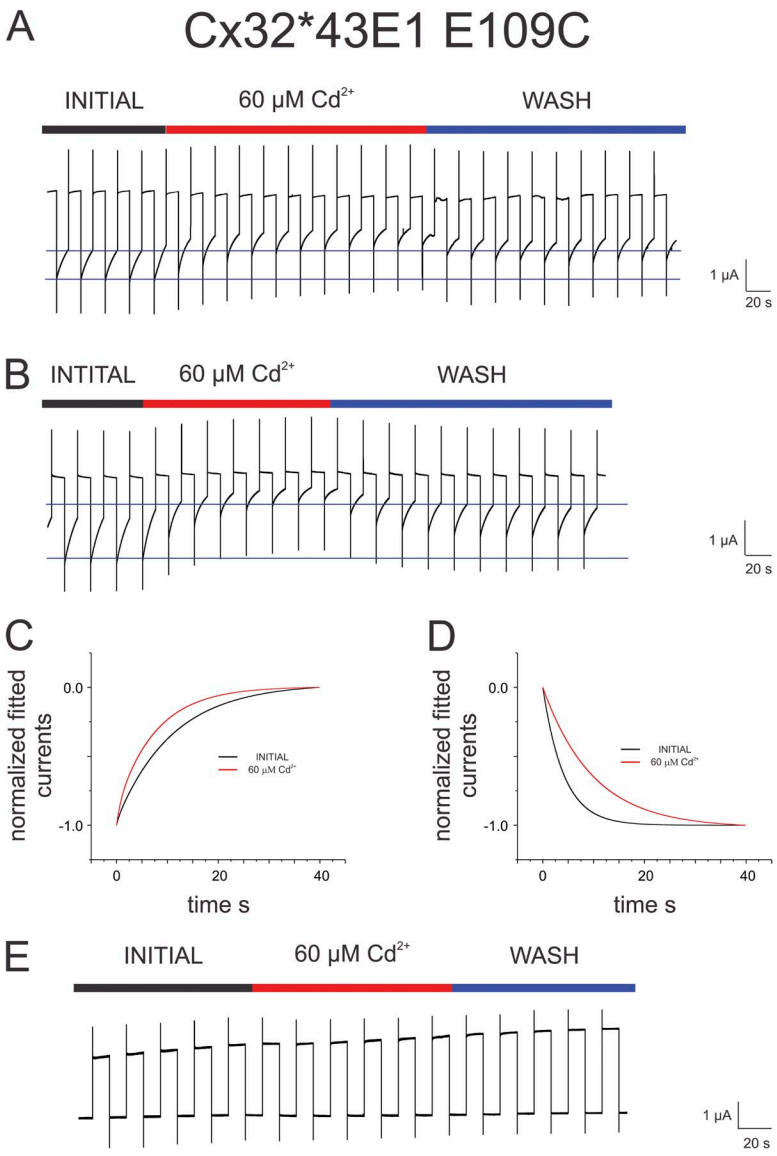

Figure 6. Cadmium stabilizes a closed state but has no effect on the open state of Cx43*43E1 L109C hemichannels. (A) A segment of a continuous current trace evoked by a train of alternating voltage polarizations from 10 mV (10 s duration) to −70 mV (10 s duration) in bath solution containing 1.8 mM $MgCl_2$. The time of perfusion with 60 µM Cd^{2+} is depicted by the red bar. (B) Same oocyte as in A, but voltage was stepped between −10 and −70 mV. (C) Plot of normalized fitted currents at steady-state of loop-gate closure at −70 mV for the current trace shown in B. Steady currents were fitted to an exponential function with two terms. Current relaxations reach steady-state faster in the presence of Cd^{2+} (red), indicating a shortening of the time constants of channel closure. (D) Plot of normalized fitted currents at steady-state of loop-gate opening at −10 mV. Steady currents were fitted to an exponential function with one term. Current relaxations reach steady-state slower in the presence of Cd^{2+}, which indicates a lengthening of time constant of channel opening. (E) Time series of current traces evoked by a train of alternating voltage polarizations from 10 mV (10 s duration) to 50 mV (10 s duration) in bath solution containing 1.8 mM $MgCl_2$. The time of perfusion with 60 µM Cd^{2+} is depicted by the red bar.

must be interpreted with caution because depolarization would tend to oppose the entrance of Cd^{2+} into the channel pore.

Conformational changes at the intracellular entrance reported by L108C

Cd^{2+} stabilizes the loop-gate closed conformation. We observed similar effects of Cd^{2+} on cysteine substitutions of L108 and N2E L108 compared with cysteine substitutions at E109. The results are summarized in Fig. 7 for Cx32*43E1 N2E L108C hemichannels. Fig. 7 (A and B) shows a substantial reduction in peak current measured at −70 mV when oocytes expressing N2E L108C are perfused with 10 and 20 µM Cd^{2+}, respectively. Peak currents obtained in the presence and absence of 20 µM Cd^{2+} are shown by arrows in the enlarged current traces shown in Fig. 7 C. These traces correspond to steady-state currents obtained initially in CsMes buffer containing 1.8 mM $MgCl_2$ (black trace), with 20 µM Cd^{2+} added (red trace), and after washing in 1.8 mM Mg^{2+} CsMes (blue trace). Normalized fitted currents indicate that the time constants of loop-gate closure at −70 mV are shortened (Fig. 7 D). Time constants of channel closure in 10, 20, and 40 µM Cd^{2+} are summarized in Table 2. The differences in τ_1 before and after addition of Cd^{2+} are statistically significant ($P > 0.05$, paired sample *t* test), whereas the changes in the shorter time constant, τ_2, are not statistically significant, although they are always lengthened after the addition of Cd^{2+}. Channel opening at −10 mV (Fig. 7 E) was best fitted by the sum of two exponential functions. In experiments adding 10 µM Cd^{2+}, the opening time constants become longer; initial $\tau_1 = 12.4$ s, $\tau_2 = 1.26$ s, and in 10 µM Cd^{2+}, $\tau_1 = 15.4$ s, $\tau_2 = 1.53$. The changes in both time constants are statistically significant ($P > 0.05$, paired sample *t* test, $n = 16$). The reductions in current observed at −10 mV in higher Cd^{2+} concentrations, coupled with the slow time course of channel opening, made fitting unreliable because of oscillations in current traces. In all cases, the stabilization of the closed state by Cd^{2+} is reversed by washing in Cd^{2+}-free solutions. We conclude that Cd^{2+} stabilizes the loop-gate closed state by bidentate coordination at L108C.

Fig. 7 F illustrates that 20 µM Cd^{2+} has little or no effect on V_j-gate closure when it is applied during a long step to 40 mV. In some experiments, we observed a small decrease in current and slowing of time constants of V_j-gating when protocols that step voltage repeatedly between 10 to 50 mV are used ($n = 5$ oocytes). This suggests that closure of V_j-gates does not cause a substantial conformational change at the cytoplasmic entrance, although as discussed for 109C hemichannels, a negative result must be interpreted with caution. Collectively, L108C reports that the intracellular entrance to the Cx32*43E1 N2E channel pore narrows substantially, from ∼15 Å in the open state to ∼10 Å with loop-gate closure. The apparent inability of cysteine substitutions to coordinate Cd^{2+} with V_j-gate closure suggests that adjacent substituted cysteine residues do not approach to within 5 Å. Therefore, the minimal pore diameter at the intracellular entrance most likely exceeds 10 Å in the V_j-closed state.

Q56C reports no conformational changes at the extracellular pore entrance

In contrast to the state-dependent formation of bidentate Cd^{2+}-thiolate bridges at L108C and E109C, 20 µM Cd^{2+} has no effect on peak currents and gating time constants of Q56C hemichannels, when records are obtained in either 1.8 mM $CaCl_2$- or 1.8 mM $MgCl_2$-containing bath solutions (Fig. 8). Notably, CaCC currents do not contribute substantially if at all to peak connexin currents in the experimental protocol that includes 1.8 mM $CaCl_2$ in the bath, as *Xenopus* oocyte CaCC currents inactivate in recordings that use trains of voltage steps between −10 and −70 mV in bath solutions containing 1.8 mM Ca^{2+} (Fig. S5). Perfusion with bath solutions containing 20 µM Cd^{2+} in either 1.8 mM Mg^{2+} or 1.8 mM Ca^{2+} does not reduce peak current nor does it change the time course of current relaxations at hyperpolarizing membrane potentials, which in the case of Cx32*43E1 Q56C hemichannels favor closure of both loop and V_j-gates (the results shown are representative of 10 oocytes). This contrasts the marked reduction in peak current and shortening of time constants of channel closure observed for L108C and E109C hemichannels with loop-gate closure. Cx32*43E1 Q56C hemichannels are labeled with Alexa Fluor 488 C5-maleimide (unpublished data), and the position of the side chain of the 56th residue is unconstrained within the open channel pore, with a pore lining probability of 1.0 in molecular dynamics simulations of Cx26 (Kwon et al., 2011) and Cx32*43E1 N2E (unpublished data) hemichannels. However, we cannot exclude the possibility that the cysteine residues becomes inaccessible when the channel adopts a closed conformation and that this results in the failure of Cd^{2+} to stabilize a closed state.

Peak currents of Cx32*43E1 Q56C hemichannels are more sensitive to [Cd^{2+}] than wild-type Cx32*43E1 hemichannels, in which peak current is only slightly reduced with 100 µM Cd^{2+} (Tang et al., 2009). 60 µM Cd^{2+} reduces peak current of Q56C hemichannels in both 1.8 mM Mg^{2+}- and 1.8 mM Ca^{2+}-containing bath solutions, but significantly, the time course of current relaxations at −70 mV are not changed in the presence and absence of added Cd^{2+} (Fig. 8, C and D). In the experimental traces obtained in 1.8 mM Mg^{2+}, the time constant of current relaxations lengthens slightly in 60 µM Cd^{2+} (Fig. 8 C). There is no difference in the time course of current relaxations when 60 µM Cd^{2+} is added to bath solution containing 1.8 mM Ca^{2+}. Peak currents

are reduced less when 40 μM Cd^{2+} is added, but again, the time course of current relaxations at −70 mV do not change from those obtained in the absence of Cd^{2+} (unpublished data). The Q56C results contrast those obtained for E109C hemichannels, where the time course of current relaxations reflecting channel closing and opening are altered substantially with addition of 60 μM Cd^{2+}. As discussed previously, the E109C and L108C results are consistent with stabilization of the loop-gate closed state. We conclude that the observed reduction in peak current of Q56C hemichannels in 40 and 60 μM Cd^{2+} is not related to

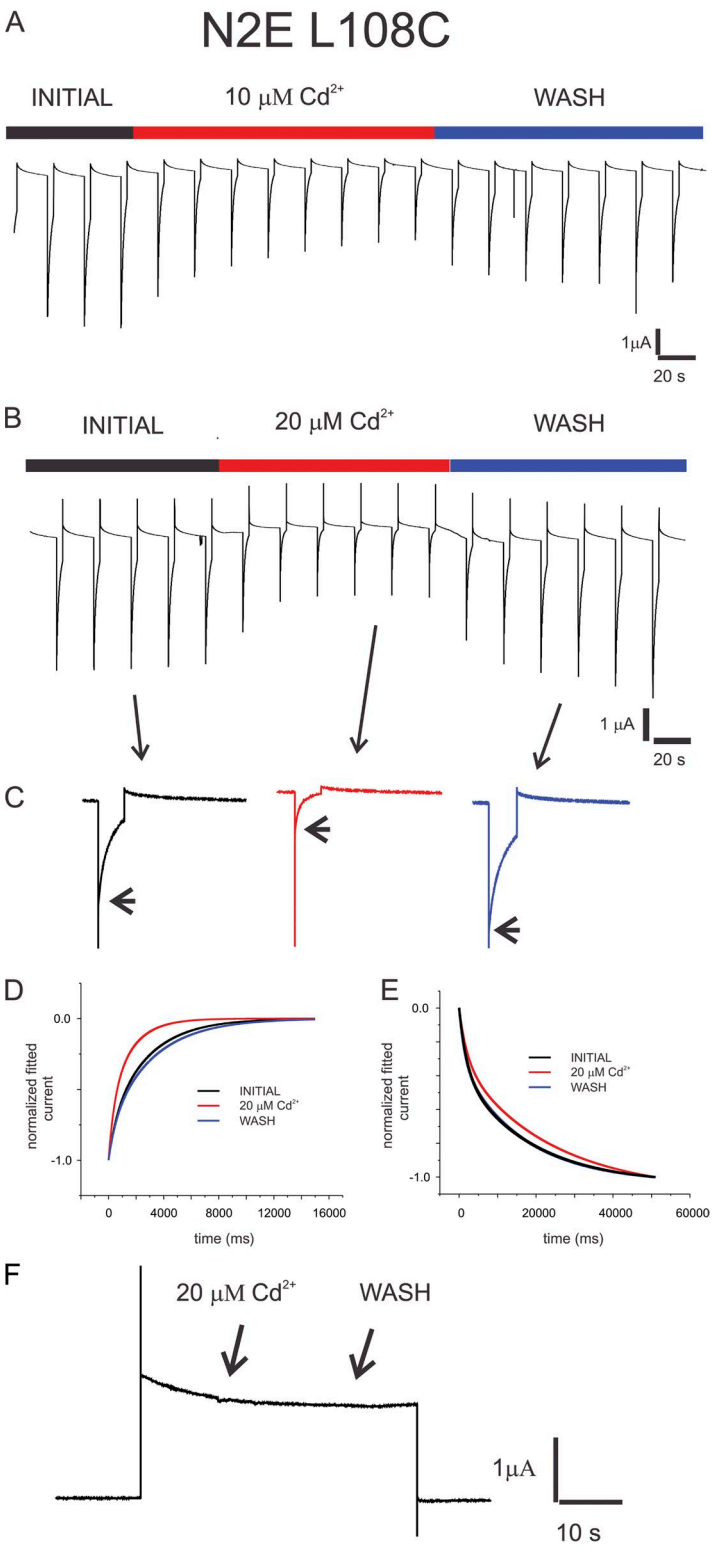

Figure 7. Cadmium stabilizes the loop-gate but not V_j-gate closed state of Cx32*43E1 N2E L108C hemichannels. (A) A segment of a continuous current trace evoked by a train of alternating voltage polarizations from −10 mV (15 s duration) to −70 mV (5 s duration). The time of perfusion with 10 μM Cd^{2+} is depicted by the red bar. (B) Same as A only with perfusion of 20 μM Cd^{2+}. (C) Expanded segments of the current trace shown in B at steady-state. Initial currents before perfusion of Cd^{2+} (black trace), steady-state current after perfusion of Cd^{2+} (red trace), and steady-state current after wash (blue trace). Arrows mark the level of peak current. Capacitive transients were not removed. (D) Plot of normalized fitted currents at steady-state of loop-gate closure at −70 mV. Steady currents were fitted to an exponential function with two terms. Current relaxations reach steady-state faster in the presence of Cd^{2+}, which indicates a shortening of the time constants of channel closure. (E) Plot of normalized fitted currents at steady-state of loop-gate opening at −10 mV. Steady currents were fitted to an exponential function with one term. Current relaxations reach steady-state slower in the presence of Cd^{2+}, which indicates a lengthening of time constant of channel opening. (F) A segment of a continuous current trace elicited by a polarization from 10 to 30 mV. Current relaxation reflects closure of V_j-gates. 20 μM Cd^{2+} was perfused at the time indicated by the arrow followed by washing with Cd^{2+}-free bath solution. Cd^{2+} had no effect on the time course to reach steady-state.

stabilization of closed states by Cd^{2+} coordination. The reduction in peak current may reflect an increased sensitivity of the Q56C hemichannel to blockage by electrostatic interactions between Cd^{2+} and the negatively charged thiol group of the substituted cysteine residue.

Because both loop and V_j-gate closure are favored at negative potentials in Q56C hemichannels, our data suggest that Q56C residues do not approach to within 5 Å, the distance that separates adjacent thiol groups necessary for bidentate coordination, in either of two voltage-dependent gating processes. Thus, the pore diameter is likely to be ≥10 Å in both the loop-gate and V_j-gate closed states. Because, the pore diameter of the open state of the Cx32*43E1 N2E is ∼14 Å, we suggest that extracellular channel entrance in the vicinity of Q56C does not undergo substantial conformational change in either 1.8 mM Mg^{2+} or Ca^{2+}, although, as we discuss previously, the results of negative results must be interpreted with caution.

To date, cysteine substitutions at the 50th residue demarcate the limit of conformational change at the extracellular end of the channel associated with loop-gate closure (Verselis et al., 2009; unpublished data). This result suggests that a bend occurs with loop-gate closure in the vicinity of the 50th residue (Fig. 9). A bend at this position would allow formation a permeability barrier by residues contained in the parahelical segment (residues 42–51), while preserving the diameter at the extracellular entrance in both undocked hemichannels and intercellular channels. Thus, the model provides a mechanism that would allow loop-gating to operate in both intercellular and undocked hemichannels; i.e., loop-gating is independent of the conformation of the portions of the extracellular loops that interact in the formation of intercellular channels. Furthermore, the similarity in the conformation of the extracellular entrance in loop-gate closed and open states suggests that the formation of intercellular channels by pairing of hemichannels that reside in the loop-gate closed conformation (required to maintain cellular integrity) can proceed without crossing a large energy barrier that would correspond to widening the extracellular channel diameter before docking with an apposed

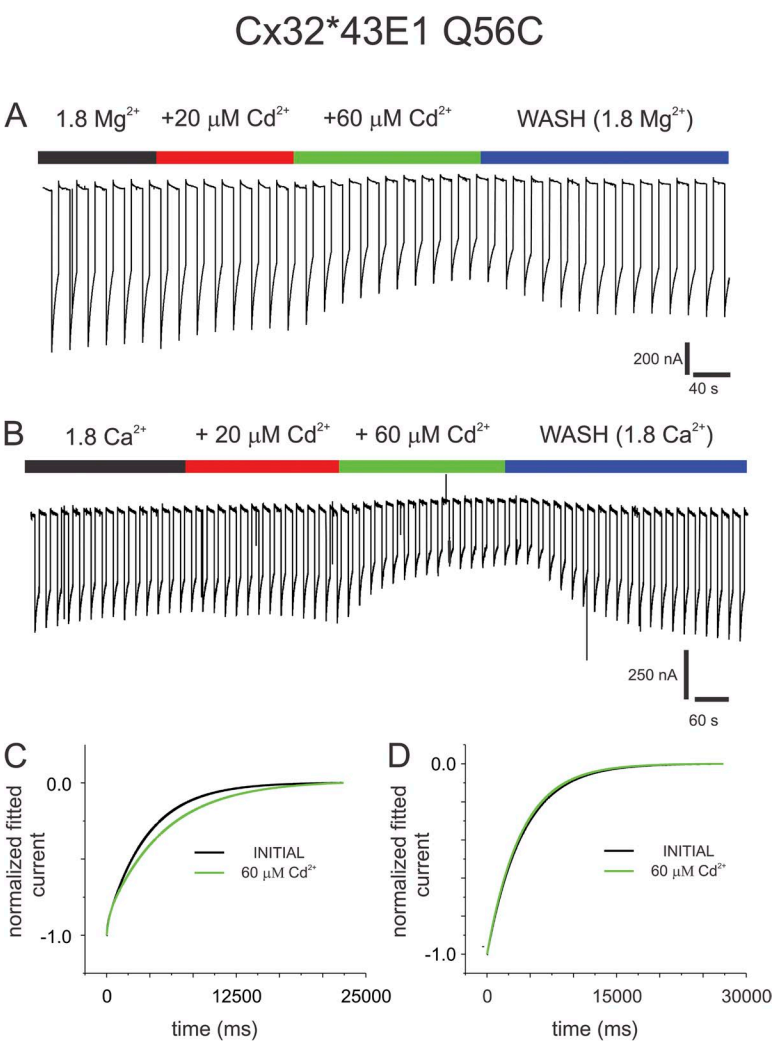

Figure 8. Cadmium does not stabilize closed conformations of Cx32*43E1 Q56C hemichannels. (A) A segment of a continuous current trace evoked by a train of alternating voltage polarizations from −10 mV (15 s duration) to −70 mV (5 s duration) in bath solution containing 1.8 mM $MgCl_2$. The time of perfusion with 20 µM Cd^{2+} is depicted by the red bar, 60 µM Cd^{2+} by the green bar. (B) Same as in A only the bath solution contained 1.8 mM $CaCl_2$. (C) Plot of normalized fitted currents at steady-state of loop-gate closure at −70 mV in 1.8 mM $MgCl_2$ bath solutions with no added Cd^{2+} (black trace) and 60 µM Cd^{2+} (green trace). Steady currents were fitted to an exponential function with two terms. Current relaxations reach steady-state more slowly in 60 µM Cd^{2+}, which indicates that the reductions in peak current shown in A do not result from the stabilization of closed states by Cd^{2+} coordination of thiol groups. (D) Plot of normalized fitted currents at steady-state of loop-gate closure at −70 mV in 1.8 mM $CaCl_2$ bath solutions with no added Cd^{2+} (black trace) and 60 µM Cd^{2+} (green trace). Steady currents were fitted to an exponential function with one term. The similarity of the time course of current relaxations in the presence and absence of Cd^{2+} indicate that the reductions in peak current shown in B do not result from the stabilization of closed states by Cd^{2+} coordination of thiol groups.

hemichannel. These aspects of intercellular channel formation are discussed in more detail by Harris (2001).

The inferred constancy of the extracellular entrance in open and voltage closed states in both Ca^{2+}- and Mg^{2+}-containing solutions differs from conformational changes reported by AFM studies of isolated Cx26 hemichannels (Müller et al., 2002). In this study, pore diameter of the extracellular entrance of isolated Cx26 hemichannels decreased markedly, from ~15 to ~5 Å in bath solutions containing 0.5 mM Ca^{2+} but not in solutions containing up to 2 mM Mg^{2+} in the absence of membrane polarization. Similar results have been reported in AFM studies of reconstituted Cx43 and Cx40 hemichannels where 1.8 mM and 3.6 mM Ca^{2+}, respectively, were required to drive most channels into a closed conformation (Thimm et al., 2005; Allen et al., 2011). If we assume (a) that the side chains of Q56C residues are accessible to the aqueous environment in the closed state and (b) that AFM studies measure pore diameter at the extracellular entrance demarcated by the 56th residue (Fig. 1), then, in a sixfold symmetrical channel, adjacent thiol groups are expected to be separated by 2.5 Å when pore diameter is 5 Å, a distance of separation that would favor the formation of tetradentate Cd^{2+}-thiolate metal bridges in a hemichannel closed by Ca^{2+}. The stabilization of this conformation by metal bridges would likely require application of chelating reagents to effect reversal. Thus, we would expect to see a marked difference in the effects of Cd^{2+} in Ca^{2+}- and Mg^{2+}-containing solutions if 1.8 mM Ca^{2+} induced at least some of the Cx32*43E1 hemichannels to close independent of voltage. However, it should be noted that the effect of Ca^{2+} and Mg^{2+} on Cx32*43E1 hemichannels has not been examined by AFM, so direct comparisons are not possible, and we do not know if higher concentrations of extracellular Ca^{2+} would gate Cx32*43E1 channels by a voltage-independent mechanism. Additionally, in contrast to AFM studies, voltage-gating of Cx26 hemichannels is sensitive to low concentrations of extracellular Mg^{2+} with an apparent K_d of ~1.8 mM (Lopez, Liu, Harris, and Contreras. 2013. 57th Annual Biophysical Society Meeting. In press.) but 2 mM Mg^{2+} does not appear to induce Cx26 channel closure in AFM studies. This suggests that the channel conformation induced by Ca^{2+} in AFM studies may not be equivalent to the conformation of loop-gates closed by voltage.

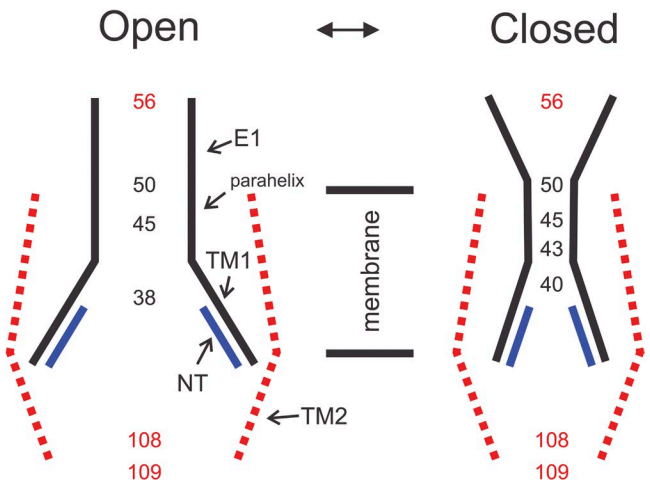

Figure 9. Schematic representation of open and loop-gate closed state of the Cx32*43E1 hemichannel. Residues reported in this study are indicated in red. Residues in black are those reported in Tang et al. (2009). The position of the 45th and 50th residues in the closed state are based on results from Cx50 hemichannels reported in Verselis et al. (2009) and unpublished studies of Cx32*43E1 hemichannels (see also Bargiello et al., 2012).

DISCUSSION

Schematic models summarizing our current knowledge of the conformation of the Cx32*43E1 hemichannel pore in open and voltage-dependent loop-gate closed states are presented in Fig. 9.

The state-dependent formation of Cd^{2+}-thiolate metal bridges in Cx32*43E1 and Cx32*43E1 N2E hemichannels containing substituted cysteines at residues L108 and E109 indicates that the pore diameter at the intracellular channel entrance narrows with loop-gate closure.

The attenuation of stabilization of the loop-gate closed state after thiol modification by MTSEA of L109C strongly suggests that backbone N and O atoms do not play a substantial role in Cd^{2+} coordination by substituted cysteines at this position. The reversal of the stabilization of the loop-gate closed state at L108C and E109C by washing with Cd^{2+}-free solutions is consistent with formation of a bidentate Cd^{2+} coordination site by thiol groups in two adjacent connexin subunits.

Given bidentate coordination and the primary involvement of the thiol group in Cd^{2+} coordination, the minimum intracellular diameter of the channel pore in the loop-gate closed state would be ~10 Å if the channel were to adopt a sixfold symmetrical structure. The mean pore diameter of the open state at the intracellular entrance is ~30 and 15 Å in the atomic models of Cx26 and Cx32*43E1 N2E, respectively, after equilibration by all atom molecular dynamics. Although substantial, the reduction in pore diameter at the intracellular entrance is unlikely to prevent ion flux given that the diameter of hydrated K^+ and Cl^- ions, 6.62 Å and 6.64 Å, respectively (Nightingale, 1959), is substantially smaller than the pore diameter in the loop-gate closed conformation.

We propose that the reduction in intracellular pore diameter is a consequence of straightening the TM1/E1 bend angle as predicted by Tang et al. (2009). Our recent analysis of the interactions that stabilize the open state of Cx26 hemichannels by molecular dynamics simulations indicate that the TM1/E1 bend angle

is stabilized by extensive van der Waals (vdW) and electrostatic networks emanating from the parahelix (Kwon et al., 2012). Straightening of the TM1/E1 bend angle with loop-gate closure is likely a consequence of the reorganization of the vdW and electrostatic interactions that accompany the conformational change in the parahelix (Kwon et al., 2012) that is induced by voltage. The TM1/E1 bend angle is also stabilized by the formation of a backbone hydrogen bond between V43hn and A39o and salt bridges formed between R32 (TM1) and E147 (TM3), as well as between K22 (TM1) and E209 (TM4). Notably, the strengths of these electrostatic interactions fluctuate over time in equilibrium molecular dynamics simulation in the absence of an applied electric field.

In contrast, the extracellular entrance to the channel pore (at the 56th residue) does not appear to undergo substantial conformational changes in either loop- or V_j-gating that reduce pore diameter to ≤10 Å, the distance at which bidentate Cd^{2+} coordination by substituted cysteines would occur, although this inference is drawn from a negative result and as such must be treated with caution. Pore diameter in the open state is ∼14–15 Å in atomic models of both Cx26 and Cx32*43E1 N2E channels. The result suggests that voltage-dependent loop-gating is independent of the conformation of the portions of the extracellular loops that interact in the formation of intercellular channels, and thus provides an explanation for the operation of loop-gating in both undocked hemichannels and intercellular channels. Although the formation of intercellular channels may modulate the expression of loop-gating, it would not be expected to prevent gating.

The results presented in this study, together with those of earlier studies (Tang et al., 2009; Verselis et al., 2009), indicate that the loop-gate permeability barrier is essentially focal, in that conformational changes in the parahelical region, specifically conformational changes at A43C, which have been shown to reduce pore diameter from ∼15–20 Å to ≤4 Å (Tang et al., 2009), are sufficient to prevent ion flux and can account for the apparent full closure of loop-gates.

The intracellular entrance to the channel pore does not appear to undergo sufficient narrowing with V_j-gate closure to allow bidentate Cd^{2+} coordination, but additional investigations are required because Cd^{2+} accessibility to cysteine substitutions at the intracellular entrance would tend to be opposed by the potentials required to initiate closure of V_j-gates. Our results suggest that pore diameter at the intracellular entrance at the TM2/CL border is >10 Å in the V_j-gate closed conformation, which is close to that of the diameter (∼15 Å) of the open Cx32 Cx32*43E1 hemichannel.

We thank Dr. Andrew Harris, University of Medicine and Dentistry, New Jersey for comments on the manuscript.

The initial stages of this study were supported by National Institutes of Health GM46889 to T.A. Bargiello. Additional support was provided by Albert Einstein College of Medicine. Computer simulations on Anton were supported by a grant (PSCA00045P) from the National Resource for Biomedical Supercomputing.

Edward N. Pugh Jr. served as editor.

Submitted: 6 June 2012
Accepted: 20 December 2012

REFERENCES

Abrams, C.K., S. Oh, Y. Ri, and T.A. Bargiello. 2000. Mutations in connexin 32: the molecular and biophysical bases for the X-linked form of Charcot-Marie-Tooth disease. *Brain Res. Brain Res. Rev.* 32:203–214. http://dx.doi.org/10.1016/S0165-0173(99)00082-X

Abrams, C.K., M.V.L. Bennett, V.K. Verselis, and T.A. Bargiello. 2002. Voltage opens unopposed gap junction hemichannels formed by a connexin 32 mutant associated with X-linked Charcot-Marie-Tooth disease. *Proc. Natl. Acad. Sci. USA.* 99:3980–3984. http://dx.doi.org/10.1073/pnas.261713499

Abrams, C.K., and S.S. Scherer. 2012. Gap junctions in inherited human disorders of the central nervous system. *Biochim. Biophys. Acta.*1818:2030–2047.http://dx.doi.org/10.1016/j.bbamem.2011.08.015

Akabas, M.H., D.A. Stauffer, M. Xu, and A. Karlin. 1992. Acetylcholine receptor channel structure probed in cysteine-substitution mutants. *Science.* 258:307–310. http://dx.doi.org/10.1126/science.1384130

Allen, M.J., J. Gemel, E.C. Beyer, and R. Lal. 2011. Atomic force microscopy of Connexin40 gap junction hemichannels reveals calcium-dependent three-dimensional molecular topography and open-closed conformations of both the extracellular and cytoplasmic faces. *J. Biol. Chem.* 286:22139–22146. http://dx.doi.org/10.1074/jbc.M111.240002

Anderegg, G., and F. Wenk. 1967. Pyridinderivate als Komplexbildner VIII Die Herstellung je eines neuen vier- und sechszähnigen Liganden. *Helv. Chim. Acta.* 50:2330–2332. http://dx.doi.org/10.1002/hlca.19670500817

Arslan, P., F. Di Virgilio, M. Beltrame, R.Y. Tsien, and T. Pozzan. 1985. Cytosolic Ca2+ homeostasis in Ehrlich and Yoshida carcinomas. A new, membrane-permeant chelator of heavy metals reveals that these ascites tumor cell lines have normal cytosolic free Ca2+. *J. Biol. Chem.* 260:2719–2727.

Bargiello, T., and P. Brink. 2009. Voltage-Gating Mechanisms of Connexin Channels. *In* Connexins. A.L. Harris and D. Locke, editors. Humana Press, New York. 103–128.

Bargiello, T.A., Q. Tang, S. Oh, and T. Kwon. 2012. Voltage-dependent conformational changes in connexin channels. *Biochim. Biophys. Acta.* 1818:1807–1822. http://dx.doi.org/10.1016/j.bbamem.2011.09.019

Barrio, L.C., T. Suchyna, T. Bargiello, L.X. Xu, R.S. Roginski, M.V. Bennett, and B.J. Nicholson. 1991. Gap junctions formed by connexins 26 and 32 alone and in combination are differently affected by applied voltage. *Proc. Natl. Acad. Sci. USA.* 88:8410–8414. http://dx.doi.org/10.1073/pnas.88.19.8410

Bennett, M.V., L.C. Barrio, T.A. Bargiello, D.C. Spray, E. Hertzberg, and J.C. Sáez. 1991. Gap junctions: new tools, new answers, new questions. *Neuron.* 6:305–320. http://dx.doi.org/10.1016/0896-6273(91)90241-Q

Berthon, G. 1995. The stability constants of metal complexes of amino acids with polar side chains. *Pure Appl. Chem.* 67:1117–1240. http://dx.doi.org/10.1351/pac199567071117

Bicego, M., S. Morassutto, V.H. Hernandez, M. Morgutti, F. Mammano, P. D'Andrea, and R. Bruzzone. 2006. Selective defects

in channel permeability associated with Cx32 mutations causing X-linked Charcot-Marie-Tooth disease. *Neurobiol. Dis.* 21:607–617. http://dx.doi.org/10.1016/j.nbd.2005.09.005

Bukauskas, F.F., and V.K. Verselis. 2004. Gap junction channel gating. *Biochim. Biophys. Acta.* 1662:42–60. http://dx.doi.org/10.1016/j.bbamem.2004.01.008

Dobrowolski, R., and K. Willecke. 2009. Connexin-caused genetic diseases and corresponding mouse models. *Antioxid. Redox Signal.* 11:283–295. http://dx.doi.org/10.1089/ars.2008.2128

Ebihara, L., X. Liu, and J.D. Pal. 2003. Effect of external magnesium and calcium on human connexin46 hemichannels. *Biophys. J.* 84:277–286. http://dx.doi.org/10.1016/S0006-3495(03)74848-6

Eggermont, J. 2004. Calcium-activated chloride channels: (un)known, (un)loved? *Proc. Am. Thorac. Soc.* 1:22–27. http://dx.doi.org/10.1513/pats.2306010

Eswar, N., B. Webb, M.A. Marti-Renom, M.S. Madhusudhan, D. Eramian, M.Y. Shen, U. Pieper, and A. Sali. 2006. Comparative protein structure modeling using Modeller. *Curr. Protoc. Bioinformatics.* Chapter 5:5.6.

Feller, S.E., and A.D. MacKerell. 2000. An improved empirical potential energy function for molecular simulations of phospholipids. *J. Phys. Chem. B.* 104:7510–7515. http://dx.doi.org/10.1021/jp0007843

Gómez-Hernández, J.M., M. de Miguel, B. Larrosa, D. González, and L.C. Barrio. 2003. Molecular basis of calcium regulation in connexin-32 hemichannels. *Proc. Natl. Acad. Sci. USA.* 100:16030–16035. http://dx.doi.org/10.1073/pnas.2530348100

Harris, A.L. 2001. Emerging issues of connexin channels: biophysics fills the gap. *Q. Rev. Biophys.* 34:325–472.

Hartzell, C., I. Putzier, and J. Arreola. 2005. Calcium-activated chloride channels. *Annu. Rev. Physiol.* 67:719–758. http://dx.doi.org/10.1146/annurev.physiol.67.032003.154341

Holmgren, M., K.S. Shin, and G. Yellen. 1998. The activation gate of a voltage-gated K+ channel can be trapped in the open state by an intersubunit metal bridge. *Neuron.* 21:617–621. http://dx.doi.org/10.1016/S0896-6273(00)80571-1

Karlin, A., and M.H. Akabas. 1998. Substituted-cysteine accessibility method. *Methods Enzymol.* 293:123–145. http://dx.doi.org/10.1016/S0076-6879(98)93011-7

Khalili-Araghi, F., V. Jogini, V. Yarov-Yarovoy, E. Tajkhorshid, B. Roux, and K. Schulten. 2010. Calculation of the gating charge for the Kv1.2 voltage-activated potassium channel. *Biophys. J.* 98:2189–2198. http://dx.doi.org/10.1016/j.bpj.2010.02.056

Khalili-Araghi, F., E. Tajkhorshid, B. Roux, and K. Schulten. 2012. Molecular dynamics investigation of the ω-current in the Kv1.2 voltage sensor domains. *Biophys. J.* 102:258–267. http://dx.doi.org/10.1016/j.bpj.2011.10.057

Krężel, A., W. Leśniak, M. Jeżowska-Bojczuk, P. Młynarz, J. Brasuñ, H. Kozłowski, and W. Bal. 2001. Coordination of heavy metals by dithiothreitol, a commonly used thiol group protectant. *J. Inorg. Biochem.* 84:77–88. http://dx.doi.org/10.1016/S0162-0134(00)00212-9

Kwon, T., A.L. Harris, A. Rossi, and T.A. Bargiello. 2011. Molecular dynamics simulations of the Cx26 hemichannel: evaluation of structural models with Brownian dynamics. *J. Gen. Physiol.* 138:475–493. http://dx.doi.org/10.1085/jgp.201110679

Kwon, T., B. Roux, S. Jo, J.B. Klauda, A.L. Harris, and T.A. Bargiello. 2012. Molecular dynamics simulations of the Cx26 hemichannel: insights into voltage-dependent loop-gating. *Biophys. J.* 102:1341–1351. http://dx.doi.org/10.1016/j.bpj.2012.02.009

Laird, D.W. 2010. The gap junction proteome and its relationship to disease. *Trends Cell Biol.* 20:92–101. http://dx.doi.org/10.1016/j.tcb.2009.11.001

Lee, J.R., A.M. Derosa, and T.W. White. 2009. Connexin mutations causing skin disease and deafness increase hemichannel activity and cell death when expressed in *Xenopus* oocytes. *J. Invest. Dermatol.* 129:870–878. http://dx.doi.org/10.1038/jid.2008.335

Maeda, S., S. Nakagawa, M. Suga, E. Yamashita, A. Oshima, Y. Fujiyoshi, and T. Tsukihara. 2009. Structure of the connexin 26 gap junction channel at 3.5 A resolution. *Nature.* 458:597–602. http://dx.doi.org/10.1038/nature07869

Moreno, A.P., M. Chanson, S. Elenes, J. Anumonwo, I. Scerri, H. Gu, S.M. Taffet, and M. Delmar. 2002. Role of the carboxyl terminal of connexin43 in transjunctional fast voltage gating. *Circ. Res.* 90:450–457. http://dx.doi.org/10.1161/hh0402.105667

Müller, D.J., G.M. Hand, A. Engel, and G.E. Sosinsky. 2002. Conformational changes in surface structures of isolated connexin 26 gap junctions. *EMBO J.* 21:3598–3607. http://dx.doi.org/10.1093/emboj/cdf365

Nightingale, E.R. 1959. Phenomenological Theory of Ion Solvation. Effective Radii of Hydrated Ions. *J. Phys. Chem.* 63:1381–1387. http://dx.doi.org/10.1021/j150579a011

Oh, S., Y. Ri, M.V. Bennett, E.B. Trexler, V.K. Verselis, and T.A. Bargiello. 1997. Changes in permeability caused by connexin 32 mutations underlie X-linked Charcot-Marie-Tooth disease. *Neuron.* 19:927–938. http://dx.doi.org/10.1016/S0896-6273(00)80973-3

Oh, S., C.K. Abrams, V.K. Verselis, and T.A. Bargiello. 2000. Stoichiometry of transjunctional voltage-gating polarity reversal by a negative charge substitution in the amino terminus of a connexin32 chimera. *J. Gen. Physiol.* 116:13–31. http://dx.doi.org/10.1085/jgp.116.1.13

Oh, S., S. Rivkin, Q. Tang, V.K. Verselis, and T.A. Bargiello. 2004. Determinants of gating polarity of a connexin 32 hemichannel. *Biophys. J.* 87:912–928. http://dx.doi.org/10.1529/biophysj.103.038448

Pfahnl, A., X.W. Zhou, R. Werner, and G. Dahl. 1997. A chimeric connexin forming gap junction hemichannels. *Pflugers Arch.* 433:773–779. http://dx.doi.org/10.1007/s004240050344

Revilla, A., C. Castro, and L.C. Barrio. 1999. Molecular dissection of transjunctional voltage dependence in the connexin-32 and connexin-43 junctions. *Biophys. J.* 77:1374–1383. http://dx.doi.org/10.1016/S0006-3495(99)76986-9

Rubin, J.B., V.K. Verselis, M.V. Bennett, and T.A. Bargiello. 1992. Molecular analysis of voltage dependence of heterotypic gap junctions formed by connexins 26 and 32. *Biophys. J.* 62:183–193, discussion :193–195. http://dx.doi.org/10.1016/S0006-3495(92)81804-0

Sánchez, H.A., G. Mese, M. Srinivas, T.W. White, and V.K. Verselis. 2010. Differentially altered Ca2+ regulation and Ca2+ permeability in Cx26 hemichannels formed by the A40V and G45E mutations that cause keratitis ichthyosis deafness syndrome. *J. Gen. Physiol.* 136:47–62. http://dx.doi.org/10.1085/jgp.201010433

Seki, A., H.S. Duffy, W. Coombs, D.C. Spray, S.M. Taffet, and M. Delmar. 2004. Modifications in the biophysical properties of connexin43 channels by a peptide of the cytoplasmic loop region. *Circ. Res.* 95:e22–e28. http://dx.doi.org/10.1161/01.RES.0000140737.62245.c5

Shaw, D.E., M.M. Deneroff, R.O. Dror, J.S. Kuskin, R.H. Larson, J.K. Salmon, C. Young, B. Batson, K.J. Bowers, J.C. Chao, et al. 2007. Anton, a special-purpose machine for molecular dynamics simulation. *SIGARCH Comput. Archit. News.* 35:1–12. http://dx.doi.org/10.1145/1273440.1250664

Shibayama, J., C. Gutiérrez, D. González, F. Kieken, A. Seki, J.R. Carrión, P.L. Sorgen, S.M. Taffet, L.C. Barrio, and M. Delmar. 2006. Effect of charge substitutions at residue his-142 on voltage

gating of connexin43 channels. *Biophys. J.* 91:4054–4063. http://dx.doi.org/10.1529/biophysj.106.085787

Sosinsky, G.E., and B.J. Nicholson. 2005. Structural organization of gap junction channels. *Biochim. Biophys. Acta.* 1711:99–125. http://dx.doi.org/10.1016/j.bbamem.2005.04.001

Tang, Q., T.L. Dowd, V.K. Verselis, and T.A. Bargiello. 2009. Conformational changes in a pore-forming region underlie voltage-dependent "loop gating" of an unapposed connexin hemichannel. *J. Gen. Physiol.* 133:555–570. http://dx.doi.org/10.1085/jgp.200910207

Thimm, J., A. Mechler, H. Lin, S. Rhee, and R. Lal. 2005. Calcium-dependent open/closed conformations and interfacial energy maps of reconstituted hemichannels. *J. Biol. Chem.* 280:10646–10654. http://dx.doi.org/10.1074/jbc.M412749200

Trexler, E.B., M.V. Bennett, T.A. Bargiello, and V.K. Verselis. 1996. Voltage gating and permeation in a gap junction hemichannel. *Proc. Natl. Acad. Sci. USA.* 93:5836–5841. http://dx.doi.org/10.1073/pnas.93.12.5836

Unwin, P.N., and P.D. Ennis. 1983. Calcium-mediated changes in gap junction structure: evidence from the low angle X-ray pattern. *J. Cell Biol.* 97:1459–1466. http://dx.doi.org/10.1083/jcb.97.5.1459

Unwin, P.N., and P.D. Ennis. 1984. Two configurations of a channel-forming membrane protein. *Nature.* 307:609–613. http://dx.doi.org/10.1038/307609a0

Vargas, E., F. Bezanilla, and B. Roux. 2011. In search of a consensus model of the resting state of a voltage-sensing domain. *Neuron.* 72:713–720. http://dx.doi.org/10.1016/j.neuron.2011.09.024

Verselis, V.K., and M. Srinivas. 2008. Divalent cations regulate connexin hemichannels by modulating intrinsic voltage-dependent gating. *J. Gen. Physiol.* 132:315–327. http://dx.doi.org/10.1085/jgp.200810029

Verselis, V.K., C.S. Ginter, and T.A. Bargiello. 1994. Opposite voltage gating polarities of two closely related connexins. *Nature.* 368:348–351. http://dx.doi.org/10.1038/368348a0

Verselis, V.K., M.P. Trelles, C. Rubinos, T.A. Bargiello, and M. Srinivas. 2009. Loop gating of connexin hemichannels involves movement of pore-lining residues in the first extracellular loop domain. *J. Biol. Chem.* 284:4484–4493. http://dx.doi.org/10.1074/jbc.M807430200

Vilariño, T., I. Brandariz, S. Fiol, J. López Fonseca, and M. Sastre De Vicente. 1993. Complexation of Cd^{2+} by cysteine at ionic strength of 0.7 m studied by differential pulse polarography. *Bulletin des Sociétés Chimiques Belges.* 102:699–707. http://dx.doi.org/10.1002/bscb.19931021104

Yellen, G. 1998. The moving parts of voltage-gated ion channels. *Q. Rev. Biophys.* 31:239–295. http://dx.doi.org/10.1017/S0033583598003448

Zonta, F., G. Polles, G. Zanotti, and F. Mammano. 2012. Permeation pathway of homomeric connexin 26 and connexin 30 channels investigated by molecular dynamics. *J. Biomol. Struct. Dyn.* 29:985–998. http://dx.doi.org/10.1080/073911012010525027